JOURNAL OF AGRICULTURAL AND FOOD CHEMISTRY

Aggregation of Casein Micelles by Interactions with Chitosans: A Study by Monte Carlo Simulations

CLAUDIO F. NARAMBUENA,[†] FERNANDO S. AUSAR,[‡] ISMAEL D. BIANCO,[‡] DANTE M. BELTRAMO,[‡] AND EZEQUIEL P. M. LEIVA*,[†]

Unidad de Matemática y Física, Facultad de Ciencias Químicas, INFIQC, Universidad Nacional de Córdoba, Ciudad Universitaria, CP 5000, Córdoba, Argentina, and Centro de Excelencia en Productos y Procesos de Córdoba (CEPROCOR), Agencia Córdoba Ciencia Pabellón CEPROCOR, CP 5164, Santa Maria de Punilla, Córdoba, Argentina

Recently, it was found that the addition of chitosan, a cationic polymer, to whole or skim milk produces the destabilization and coagulation of casein micelles which takes place without modifications in the milk pH or in the stability of most of the whey proteins. In the present work, Monte Carlo simulations are employed to show that the phase separation of casein micelles induced by chitosan can be explained by a depletion mechanism, where an effective attraction between the casein micelles is induced by the presence of chitosan molecules. This interaction is described on the basis of Vrij's model, where the depletion of polymer from the gap between neighboring casein micelles originates an effective attractive interaction that leads to a phase transition. This model, that considers volume restriction effects, accounts for several qualitative and even quantitative aspects of the experimental data for the coagulation of casein through chitosan addition.

KEYWORDS: Casein micelles; chitosan; depletion mechanism; Monte Carlo simulation

INTRODUCTION

The caseins are, quantitatively, the most important protein components of the milk (*1*). This protein complex, known as micelle, has been thoroughly investigated and can be considered as a highly hydrated spherical particle, with diameters (σ_c) ranging between 20 and 300 nm, resulting in a log-normal distribution with an average diameter of 200 nm (*2*, *3*). The micelle is formed of four protein types, α_{s1}, α_{s2}, β, and κ-casein. A higher amount of κ-casein is found on the surface, forming a specific area denominated glycomacropeptide (GMP), consisting in a brush of negatively charged polyelectrolyte that stabilizes the micelle sterically. This polyelectrolyte layer is responsible for the high stability of the casein micelles by means of steric and electrostatic interactions that prevent flocculation (*4*, *5*). The stability of the layer depends on both the density of chains and the charge density along the chain. When the chain collapses, because of either a decrease in the charge density (i.e., via pH decrease) or in the density of chains (action of rennet), or both, the casein micelles lose stability and coagulate (*6*).

The micelles can be destabilized through interaction with polysaccharides (*7*−*9*). In this respect, the interaction between casein micelles and chitosan, a cationic copolymer formed of β-glucosamine and *N*-acetylglucosamine, has been recently investigated (*10*). In this work, it was shown that the addition of chitosan to milk produces the destabilization and coagulation of the casein micelles without a concomitant pH change or loss of whey proteins. It was also concluded that electrostatic interactions were not determinant in the formation of the complex between chitosan molecules (HMWC, MMWC, and LMWC) and casein micelles because the addition of high NaCl concentrations was unable to prevent coagulation or dissociate the aggregates (*10*). The studies about the influence of temperature in the chitosan−casein complex formation showed that CHOS−casein interaction was temperature independent, while for the other chitosan−casein complex, the interactions increase with the temperature. However, it was suggested that this effect was related to a reduction of the viscosity of the polymer rather than a change in the enthalpy of the reaction. The optical microscopy analysis of the complexes formed showed that their size increases with the chitosan molecular weight. Fermented milk gels and rennet curds are particle gels formed of casein micelles. As it is well known that textural properties of gelled products are perceived by consumers as an important attribute determining food quality, extensive work is being conducted on different aspects relative to these issues to understand, and eventually control, how these aggregates are structured and held together.

The present work is based on the computer simulation of the interaction of casein micelles mediated by chitosan, by means of a model formulated by Vrij, who showed that attractive interactions are induced between colloids in colloid−polymer mixtures because of the presence of the nonadsorbing polymers (*11*).

* Author to whom correspondence should be addressed. E-mail: eleiva@mail.fcq.unc.edu.ar.
[†] Universidad Nacional de Córdoba.
[‡] Centro de Excelencia en Productos y Procesos de Córdoba.

10.1021/jf049202v CCC: $30.25
Published on Web 12/22/2004

THEORY

The destabilization of colloidal systems, such as casein micelles, through polysaccharides has been discussed in a general framework by Vrij (*11*). This phenomenon is caused by the expulsion of polysaccharides from the interstitial space between colloidal particles because of restricted volume and osmotic effects. The two mechanisms can be explained as follows: in the first case, the added polymer molecules lose configurational entropy when they penetrate the space between the interacting micelle surfaces. In the second case, the segments of the added polymer interact with segments of the polymer chains that belong to the micelle, leading to an increase in the local "osmotic pressure". Depending on the added polymer size in relation to the size of the polymer layer attached to the particles, one of these mechanisms of polymer depletion prevails (*11*).

In Vrij's colloid−polymer model, the colloids are represented as hard spheres with diameter σ_c, whereas the polymer coils are described as interpenetrating, noninteracting particles as regards their mutual interactions (*11*). However, the polymers are excluded by a center-of-mass distance of $(\sigma_c + \sigma_p)/2$ from the colloids, where σ_p, the diameter of the polymer coil, is given by $\sigma_p = 2R_g$ with R_g being the radius of gyration of the polymer. The author derived an effective potential $U(r)$ between colloidal particles that was proportional to the overlap volume V_{overl} and to the osmotic pressure Π_p according to

$$\begin{aligned} U(r) &= \infty \qquad 0 < r < \sigma_c \\ &= V_{overl}\Pi_p \qquad \sigma_c < r < (\sigma_c + \sigma_p) \\ &= 0 \qquad r > (\sigma_c + \sigma_p) \end{aligned} \tag{1}$$

where V_{overl} depends on the distance r between the particles and is given by

$$V_{overl}(r) = \frac{1}{6}\pi(\sigma_c + \sigma_p)^3\left[1 - \frac{3r}{2(\sigma_c + \sigma_p)} + \frac{r^3}{2(\sigma_c + \sigma_p)^3}\right] \tag{2}$$

For the osmotic pressure of the polymer solution, Vrij used the limiting Van't Hoff's law: $\Pi_p = n_p RT$ with $n_p = C_p/M_W$, where C_p and M_W are the polymer concentration and the molecular weight, respectively.

However, in the present research, simulation results are compared with experimental data obtained previously, where the σ_p values were relatively large and excluded-volume effects are expected to be substantial (*10*). For this reason, an expression for the osmotic pressure that accounts the free volume $V_{free}(r_c)$ available for the motion of the polymer chain has been used (*12*). Since $V_{free}(r_c)$ depends on the colloid particle positions, collectively denoted by r_c, the $U(r)$ potential has an implicit many-body nature. $V_{free}(r_c)$ may be written in terms of the mutual overlap of the excluded-volume shells of all the colloid particles.

Lekkerkerker and co-workers have replaced $V_{free}(r_c)$ by its average value in the corresponding unperturbed system of colloidal particles, so that $V_{free}(r_c) = \alpha \cdot V$, where α is the free-volume fraction that depends only on the colloid volume fraction $\phi_c = [\pi(\sigma_c)^3 N_c]/6$ and on the ratio $\xi = \sigma_p/\sigma_c$. All the information concerning the interactions between colloid and polymer is now contained in the variation of α with ϕ_c. An approximate expression for α is the one proposed by Lekkerkerker (*12*), given by $\alpha = (1 - \phi)\exp[-A\gamma - B\gamma^2 - C\gamma^3]$, where $A = 3\xi + 3\xi^2 + \xi^3$, $B = 9/2\ \xi^2 + 3\xi^3$, $C = 3\xi^3$, and the full expression for the osmotic pressure (*12*) follows the equation

$$\Pi_p = \left(1 - \frac{\phi_c}{\alpha}\frac{d\alpha}{d\phi_c}\right)n_p RT \tag{3}$$

MATERIALS AND METHODS

Computer Simulations. The simulation system consisted of 1000 particles interacting via the potential given in eq 1. The casein molecules were assigned a 200-nm diameter (σ_c) and the diameter of the polymers σ_p in eq 2 was assumed to be equal to twice the gyration radius (**Table 1**). The particles were located into a cubic simulation box with periodic boundary conditions with a volume fraction of casein micelle $\phi_c = 0.1$, which is close to the concentration in cow milk. The side of the box was $L = 3472.5$ nm. The equilibrium properties of the system were evaluated by computer simulations devised according to the Metropolis Monte Carlo (MC) algorithm (*13*). The particles were initially positioned at random within the simulation box, avoiding overlapping, since these are represented as hard spheres, according to eq 1. The algorithm employed allowed for single particle displacement, as is usual in liquid-state simulations (*14*, *15*). The displacement of a particle is accepted with the probability $\{1, \exp(-\Delta U/kT)\}$ where ΔU denotes the change of the potential energy between the initial and the final configuration, k is Boltzman's constant, and T is the absolute temperature. The system was allowed to equilibrate for 100 000 MC steps, following then the evaluation run during 100 000 MC steps. Chitosans of four different molecular weights M_w were employed in the simulations (**Table 1**). The data of **Table 1** correspond to the same chitosans used in our previous experimental work (*10*).

The diameters of the chitosan particles, required to calculate Vrij's pair potentials, were calculated from the gyration radius according to the equation $R_g = 7.5 \times 10^{-2} M_w^{0.55}$, as proposed by Berth and Dautzenberg (*16*).

Materials and Reagents Employed in Previous Experimental Work Referenced Here. The structural information corresponds to high MW chitosan (HMWC), medium MW chitosan (MMWC), and low MW chitosan (LMWC), with approximately 80% deacetylation from Aldrich (Milwaukee, WI) and chitosan oligosaccharide (CHOS) that contains a mix of di-, tri-, tetra-, penta-, and exasaccharide from Kimitsu Chem. Ind. (Tokyo, Japan). Stock solutions of chitosans were prepared in 100 mM acetate buffer, pH 5.9. Whole and skim bovine milks were from local commercial sources in the province of Córdoba, Argentina. Rennet from Mucor Miehei and different phosphorylated and dephosphorylated caseins were obtained from Sigma Chemical Co. (St. Louis, MO). All other reagents used were of analytical grade.

RESULTS AND DISCUSSION

Figure 1 shows the pair potentials of the casein micelles in the presence of different concentrations of chitosan at 300 K. Considering that these curves have been normalized by the casein diameter σ_c, it can be observed that in the CHOS the potential is rather short-ranged as compared with the diameter of the micelle. On the other hand, for MMWC and HMWC the interaction range may be as large as twice σ_c. The polymer concentration required to obtain a given magnitude of the potential is considerably lower in the HMWC than in the remaining cases. The polymer-induced attraction between micelles, which in the present studies reaches up to 20 kT, is expected to lead to a phase separation (where one phase is rich in micelles and the other one in polymers).

The structure of the system may be characterized by the radial distribution function $g(r)$, that provides information on the density of micelles at a distance r from a given micelle, normalized to one for uncorrelated (distant) micelles, that is, at long distances. **Figure 2** shows $g(r)$ obtained from simulations with different chitosan types, at a given concentration and 300 K, where structuring of the system becomes evident. Because of the hard core repulsion between micelles, the radial distribution function $g(r)$ becomes zero at short distances. In all cases, an intense peak becomes evident between 1.0 σ_c and 1.1 σ_c,

Table 1. Relevant Characteristics of Chitosan Simulated in This Work

chitosan	mol wt, M_w (kDa)	gyration radius, R_g (nm)	$\xi = \sigma_p/\sigma_c$[e]	ϕ_p^*[f]
CHOS[a]	0.72	2.8	0.028	0.11
LMWC[b]	80	37.3	0.373	0.35
MMWC[c]	400	90.4	0.904	0.28
HMWC[d]	600	113.0	1.130	0.24

[a] CHOS: chitosan oligosaccharides. [b] LMWC: low molecular weight chitosan. [c] MMWC: medium molecular wight chitosan. [d] HMWC: high molecular weight chitosan. [e] $\sigma_p = 2R_g$ and $\sigma_c = 200$ nm. [f] ϕ_p^* is defined as the value of the volume fraction of the polymer at which the concentration of free casein is one-half of the value in the absence of polymers (see Results and Discussion).

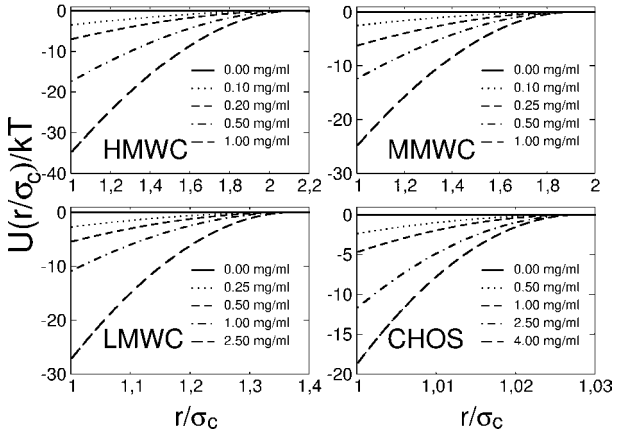

Figure 1. Effective pair potentials for the interaction between casein micelles in the presence of chitosan at 300 K and at different concentrations.

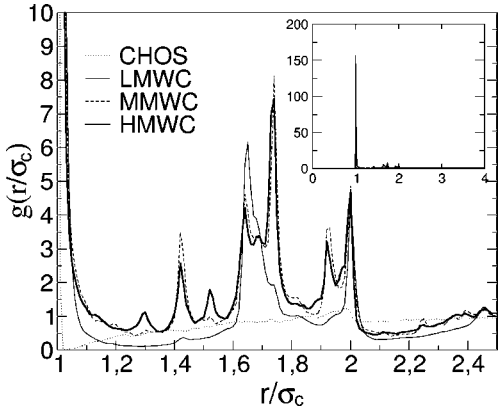

Figure 2. Radial distribution functions $g(r)$ for casein micelles in the presence of different chitosan types, at a concentration of 2.50 mg/mL and 2.00 mg/mL for CHOS and for the remaining polymers, respectively, at 300 K. The inset shows $g(r)$ in a larger scale, where the first peak becomes evident.

which is accompanied by a set of peaks between 1.3 σ_c and 2.0 σ_c that are practically absent in CHOS. The peaks become more intense as the chitosan molecular weight increases. The intensity of the peak close to 1.10 σ_c was taken as a criterion for the equilibration of the simulations. This showed the stronger changes within the first 100 000 MC steps. The configurations corresponding to this equilibration stage were discarded for the evaluation of the properties reported here.

An important quantitative value reported in our previous experimental work (*10*) was the amount of protein that remains soluble after interaction with various chitosans at 277, 300, and 343 K. The coagulation process for CHOS shows little temperature dependence, whereas for LMWC, MMWC, and HMWC the coagulation became more efficient at higher temperatures, ruling out an enthalpy-driven process for the aggregation observed. A microscopic analysis of casein micelles aggregates showed that the sizes of the micelle clusters increase with the molecular weight of chitosan. To attempt a correlation between these previous experimental results and the present simulations, a criterion must be used to define the coagulation of the micelles. Thus, we have chosen to define the connectivity between the micelles. As the first peak in **Figure 2** occurs between σ_c and 1.1 σ_c, it was assumed that two micelles connect when the distance between their centers is equal to or lower than 1.10 σ_c. Furthermore, it was assumed that a micelle belongs to a given cluster if it is connected to it either directly or through other micelles. According to this criterion, when a simulation was performed in the absence of chitosan, the 1000 particles were distributed into 741 monomers, 98 dimers, 18 trimers, 1 tetramer, and 1 pentamer. From these results, where the system is not perturbed by an attractive potential, it is evident that the presence of dimers and trimers is usual in a noncoagulated system. According to this, we define the fraction of free micelles as

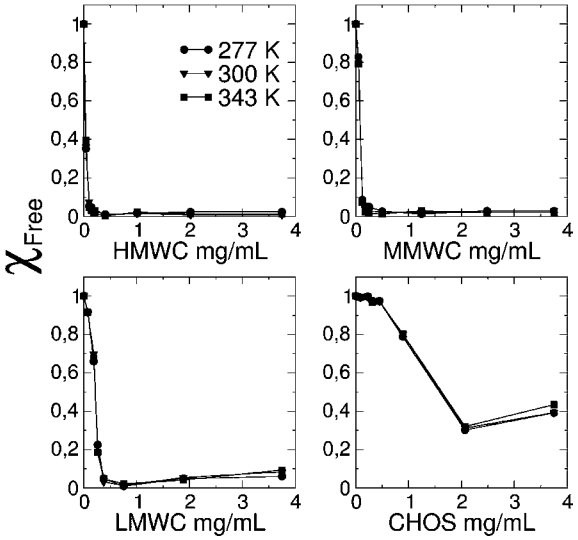

Figure 3. Fraction of free casein micelles χ_{free} as a function of the chitosan concentration employed for the coagulation at different temperatures.

$$\chi_{free} = \frac{np}{np_0}$$

where np denotes the total number of micelles that are in the form of monomers, dimers, and trimers in the system with an attractive effective potential, and np_0 is analogous for the system without polymer addition (that is, with the hard core potential, resulting in $np_0 = 991$ in the example given above).

Figure 3 shows χ_{free} as a function of the chitosan concentration employed for coagulation at different temperatures. It is evident from the figure that the fraction of free micelle is highly sensitive to the concentration of polymer added within the concentration range experimentally employed in our previous work (*10*). Furthermore, for a given mass of polymer added, the high molecular weight polymers seem to be more efficient for the coagulation process. A statistical analysis of the uncertainties of the present results shows that typical errors in χ_{free} are about 2×10^{-2}, so that they are smaller than the size of the symbols employed for the plots in **Figure 3**. The same is true for the results presented below in **Figure 4**.

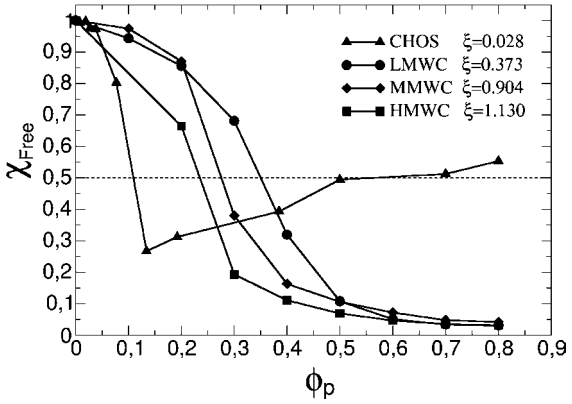

Figure 4. Fraction of free casein micelles χ_{free} at 300 K as a function of the volume fraction occupied by the polymer ϕ_P. The values of ξ, denoting the ratio of polymer to micelle radius, are given in the inset.

Table 2. Critical Concentration of Chitosan, c_c, Required To Reduce the Free Casein to Half of the Value in the Absence of Polymers[a]

		$c_{c,exptl}$			
chitosan	c_c simulation	343 K	300 K	277 K	$c_p^*\alpha$
CHOS	1.71	1.93	1.93	2.14	11.59
LMWC	0.22	0.54	1.07	1.21	0.46
MMWC	0.08	0.54	1.25	1.90	0.09
HMWC	0.03	0.54	1.25	2.25	0.05

[a] Results from the present simulations and experiments (*10*) in mg/mL. $c_p^*\alpha$ is the critical concentration at which the polymer coil begin to overlap, α is the free-volume fraction, so that $c_p^*\alpha$ is the free-volume corrected critical concentration (for more details see Results and Discussion).

The critical concentration of chitosan c_c will be defined as the concentration required to reduce the free casein to one-half of the value in the absence of polymers. The values of c_c obtained from the simulation are compared with experimental results in **Table 2**. While the c_c value for CHOS is in excellent agreement with the experimental results, the c_c values for the remaining polymers are lower than the corresponding experimental ones. The dependence on the temperature shown by the theoretical curves is lower than that of the experimental ones (*10*). This indicates that the mechanism proposed in the present work would be the main cause of aggregation. However, certain factors indicate that other types of interactions, besides the depletion mechanism, are present. The strong effect of temperature on the experimental profiles of soluble protein in relation to the concentration of chitosan added may be caused either by kinetic effects or by some kind of interaction which is not accounted for in the model used in this work. Two interactions absent in this model are chitosan adsorption onto the micelle surface and the interaction between chitosan chains. The former interaction may influence the coagulation process favorably, as it may contribute to the collapse of the GMP brush, and facilitate the interaction among micelles. In any case, it is clear from the simulations that the presence of this interaction is not essential for coagulation to occur. The second type of interaction, self-interaction among chitosans, is now considered.

Much of the knowledge concerning polymer solution is derived from the scaling arguments pioneered by de Gennes (*17*). These suggest that the behavior of a polymer solution in the dilute regime, where the polymer concentration is $c_p < c_p^*$, differs from that in the semidilute regime, where $c_p/c_p^* > 1$; c_p^* represents the overlapping concentration, the critical concentration at which the polymer coils begin to overlap, and is defined as $c_p^* = 3M_w/[4\pi(R_g)^3N_A]$ where N_A is Avogadro's number. While in the dilute regime, the different polymer coils do not interact; this is not the case in the semidilute regime, where interactions are present. To define a specific system, it must be considered that the available volume for the polymer is $V_{free} = \alpha V$. Thus, the overlapping concentration must refer to this volume. In other words, the overlapping concentration will be αc_p^* (**Table 2**) rather than c_p^*. The αc_p^* values in **Table 2** show that only CHOS can be considered to be in the dilute regime, so that in all the other cases some interaction between polymers is expected. In fact, the concentration in the LMWC, MMWC, and HMWC employed in the experiments are above the overlapping concentration corrected by the free volume (**Table 2**), and it is experimentally proved that chitosan can form hydrophobic self-aggregates at a concentration in the order of the overlapping concentration (*18*, *19*). This could explain the decrease in the efficiency of chitosans (except CHOS) for casein coagulation at lower temperatures, since chitosan self-aggregates are expected to become more stable as temperature decreases. A hypothesis, to be experimentally proved, is that the use of either chitosans or an analogous polymer which has a lower self-aggregation would favor the coagulation process as there would be a higher availability of the polymer to cause depletion.

Considering that the volume fraction of the polymer is given by $\phi_p = [\pi(\sigma_p)^3N_p]/(6\ V)$, with $N_p = (C_p/M_W)N_A$, (N_A, Avogadro's number), the fraction of free micelles as a function of the volume fraction of the polymer can be plotted (**Figure 4**). As before, a critical fraction ϕ_p^* can be defined as the value of ϕ_p at which the concentration of free casein is one-half of the value in the absence of polymers. These ϕ_p^* values are reported in **Table 1**. While CHOS seems to be more efficient in producing coagulation at lower volume fractions, this effect appears to be reversed at higher volume fractions. This result could be partially an artifact, consequence of the criterion chosen to define soluble casein as monomers, dimers, and trimers. Since the effective interaction generated by CHOS is relatively short-ranged as compared with that induced by the other chitosans, many dimers and trimers occur that are counted as free casein particles. Since the mobility of these particles is much lower than that of single casein units, large aggregates are not produced during the simulation. On the other hand, this effect could also occur in the experiment if smaller casein clusters are counted as soluble proteins.

The simulations also provide information on the relative distribution of different sizes of micelle clusters *f(N)* where *N* is the aggregation number. **Figure 5** shows the frequency function *f*(*N*) of cluster sizes found in the simulations for a concentration of 2.50 mg/mL in CHOS and 2.00 mg/mL in the remaining polymers. In agreement with the experimental observations (*10*), for higher molecular weights of the polymer the frequency of cluster sizes *f*(*N*) shifts toward higher aggregation numbers. The fact that larger aggregates are obtained as the molecular weight of the chitosan increases can be simply explained as a result of the depletion mechanism. Attractive potentials for CHOS are short-ranged and have a lower magnitude than those for the remaining chitosans (see **Figure 1**). Such short-ranged potentials cause the formation of clusters with low aggregation number. This is because micelles must be very close to one another to "perceive" the attractive potential, which accounts for the predominant formation of dimers and trimers whose translation is reduced in relation to that of monomers. Thus, it is relatively unlikely that two clusters with large aggregation numbers meet to generate an even larger cluster. For the remaining chitosans, attractive potentials are

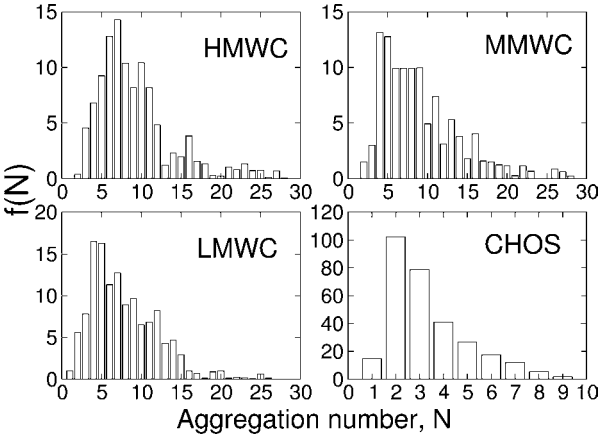

Figure 5. Cluster size distribution of casein micelles in the presence of chitosans of different molecular weights at 300 K. Concentration of 2.50 mg/mL and 2.00 mg/mL for CHOS and for the remaining polymers, respectively.

relatively long-ranged. As the range and magnitude parameters increase, clusters with a higher aggregation number are obtained, since after the formation of a dimer or a trimer the potential is strong enough in range and magnitude to attract other clusters and to cause the size distributions observed in the simulations.

It is generally accepted that networks built of casein micelles are the result of aggregation brought about by modifying or reducing the repulsive interaction energy (electrostatic and steric) between the stable micelles (*6*). In this context, it was initially proposed that casein aggregation induced by chitosan involves both electrostatic and hydrophobic interactions that contribute energetically to the association (*10*). On the basis of the characteristics of the system and the experimental results available, it is assumed that a depletion mechanism may be the main reason for the aggregation of casein micelles in the presence of chitosan.

In conclusion, it can be affirmed that the coagulation of casein through chitosan addition can be explained in first approximation by a depletion mechanism, in which the systems tend to increase the free volume for the polymer on the basis of an effective attractive interaction between the casein micelles. Kinetic effects, interactions leading to chitosan adsorption on casein, or association between chitosan molecules unaccounted for in the present model may be responsible for the stronger effect of temperature on the fraction of free casein micelles after coagulation. Futures studies will be addressed to account properly for these variables.

ABBREVIATIONS USED

GMP, glycomacropeptide; CHOS, chitosan oligosaccharides; LMWC, low molecular weight chitosan; MMWC, medium molecular weight chitosan; HMWC, high molecular weight chitosan.

ACKNOWLEDGMENT

Language assistance by Karina Plasencia is gratefully acknowledged.

LITERATURE CITED

(1) Walstra, P.; Jenness, T. *Dairy chemistry and physics*; John Wiley and Sons: New York, 1984.
(2) de Kruif, C. G. Supra-aggregates of casein micelles as a prelude to coagulation. *J. Dairy Sci.* **1998**, *81*, 3019−3028.
(3) Morris, G. A.; Foster, T. J.; Harding, S. E. Further observations on the size, shape, and hydration of casein micelles from novel analytical ultracentrifuge and capillary viscometry approaches. *Biomacromolecules* **2000**, *1*, 764−767.
(4) Dalgleish, D. G. Casein micelle as colloids: Surface structures and stabilities. *J. Dairy Sci.* **1998**, *81*, 3013−3018.
(5) de Kruif, C. G. Casein micelle interactions. *J. Dairy Sci.* **1999**, *9*, 183−188.
(6) Tuinier, R.; de Kruif, C. G. Stability of casein micelles in milk. *J. Chem. Phys.* **2002**, *117*, 1290−1295.
(7) Tuinier, R.; de Kruif, C. G. Phase behaviour of casein micelles/exocellular polysaccharide mixtures: Experiment and theory. *J. Chem. Phys.* **1999**, *110*, 9296−9304.
(8) Tuinier, R.; ten Grotenhuis, E.; Holt, C.; Timmins, P. A.; de Kruif, C. G. Depletion interaction of casein micelles and an exocellular polysaccharides. *Phys. Rev. E* **1999**, *60*, 848−856.
(9) Tuinier, R.; ten Grotenhuis, E.; de Kruif, C. G. The effect of depolymerised guar gum on the stability of skim milk. *Food Hydrocolloids* **2000**, *14*, 1−7.
(10) Ausar, S. F.; Bianco, I. D.; Badini, R. G.; Castagna, L. F.; Modesti, N. M.; Landa, C. A.; Beltramo, D. M. Characterization of casein micelle precipitation by chitosan. *J. Dairy Sci.* **2001**, *84*, 361−369.
(11) Vrij, A. Polymers at interfaces and the interactions in colloidal dispersions. *Pure Appl. Chem.* **1976**, *48*, 471−483.
(12) Lekkerkerker, H. N. W.; Poon, W. C. K.; Pusey, P. N.; Stroobants, A.; Warren, P. B. Phase behaviour of colloids + polymer mixtures. *Europhys. Lett.* **1992**, *20*, 559−564.
(13) Metropolis, N.; Rosenbluth, A. W.; Rosenbluth, M. N.; Teller, A. H.; Teller, E. Equation of state calculations by fast computing machines. *J. Chem. Phys.* **1953**, *21*, 1087−1092.
(14) Allen, M. P.; Tieldesley, D. J. *Computer Simulation of Liquids*; Oxford Science Publications: Oxford, U.K., 1992.
(15) Frenkel, D.; Smit, B. *Understanding Molecular Simulation*; Academic Press: San Diego, CA, 1996.
(16) Berth, G.; Dautzenberg, H. The degree of acepylation of chitosans and its effect on the chain conformation in aqueous solution. *Carbohydr. Polym.* **2002**, *47*, 39−51.
(17) de Gennes, P. G. *Scaling concepts in Polymer Physics*; Cornell University Press: Ithaca, NY, 1979.
(18) Buhler, E.; Rinaudo, M. Structural and dynamical properties of semi-rigid polyelectrolyte solutions: A light-scattering study. *Macromolecules* **2000**, *33*, 2098−2106.
(19) Philippova, O. E.; Volkov, E. V.; Sitnikova, N. L.; Khokhlov, A. R.; Desbrieres, J.; Rinaudo, M. Two types of hydrophobic aggregates in aqueous solutions of chitosan and its hydrophobic derivative. *Biomacromolecules* **2001**, *2*, 483−490.

Received for review May 18, 2004. Revised manuscript received October 21, 2004. Accepted November 3, 2004. Financial support from Secretaría de extensión Universitaria U.N.C., CONICET, Agencia Córdoba Ciencia, Secyt U.N.C., Program BID 1201/OC-AR PICT 06-12485 is gratefully acknowledged.

JF049202V